Induction heated hydrogen production
EUDP project no.: 64013-0511
Final report

Final report

1.1 Project details

Project title	Induction heated hydrogen production
Project identification (program abbrev. and file)	EUDP project no.: 64013-0511
Name of the program which has funded the project	Brint og Brændselsceller
Project managing company/institution (name and address)	Haldor Topsoe A/S Haldor Topsøes Allé 1 2800 Lyngby
Project partners	Teknologisk Institut
CVR (central business register)	41853816
Date for submission	

1.2 Short description of project objective and results

The project had the objective to investigate and demonstrate that inductive heating of a catalyst could be used for hydrogen production by steam reforming. Induction heating is expected to be more effective for a catalytic steam reformer because heat is provided where the catalytic reactions occurs. For this purpose, a catalyst with a ferromagnetic active phase should be developed. This was done in two different catalyst/magnetic susceptor configurations: a catalyst with a magnetic nanoparticle system and a large magnetic susceptor surrounded by catalytic material.

The first version was achieved using a ceramic carrier with active Co-Ni nanoparticles. It was shown to have sufficient activity and a sufficient high Curie temperature to obtain inductive heating and steam reforming at above 800°C. Fast response times in the order of seconds was achieved, but the energy transfer efficiency to the nanoparticles was low. The second configuration was large cobalt rods surrounded with catalytic material. This configuration similar showed fast response and achieved high temperatures and thereby high conversions, but additionally achieved high (60%) energy transfer efficiency.

In this work, it was shown that the energy transfer by hysteresis of the material alone is not sufficient to obtain the desired conversions, heat from eddy currents is needed as well, and for this, we need to develop susceptor materials with high Curie temperatures and adaptable for ceramic coats to contain the catalytic phase.

Despite the challenges, an economic analysis showed that the concept was competitive with electrolysis when using the consumption figures measured in the laboratory setup and overall the project consequently showed induction-heated steam reforming as a prospective future method for hydrogen production.

Projektet havde til formål at undersøge og demonstrere en katalysator til steam reforming, der kan opvarmes ved brug af induktion. Dette vil give en mere effektiv proces, da varmen leveres, hvor den skal benyttes til den katalytiske reaktion. Til dette formål skal der bruges en katalysator, der foruden katalytisk aktivitet også er ferromagnetisk.

To forskellige konfigurationer af katalysator og ferromagnetisk susceptor blev udviklet: en katalysator med magnetiske nanopartikler og magnetisk susceptor blandet op i det katalytiske materiale. Den første består af en katalysator baseret på Co-Ni nanopartikler, der både har

tilstrækkelig Curie temperatur og katalytisk aktivitet. Vi har vist, at vi opnår meget korte responstider med dette system. Desværre var energieffektiviteten i disse forsøg forholdsvis lav da systemet var begrænset til kun at modtage energi via hystereseopvarmning. For at opnå en bedre energieffektivitet er det nødvendigt at benytte materialer, hvor der afsættes eddy currents fra induktionsfeltet. Hertil blandes større koboltstænger med en nedknust katalysatorbærer. Dette system opnåede en effektivitet på 60%.

Selvom der stadig er udfordringer, viser arbejdet i dette projekt, at induktionsopvarmet steam reforming har potentiale som en fremtidig produktionsmetode til brint, som kan være konkurrencedygtig med produktion af brint ved brug af elektrolyse.

1.3 Executive summary

Induction-heated hydrogen production was shown to be possible with an efficiency as high as 60% yielding a lower energy requirement per hydrogen molecule than electrolysis. The results formed the basis of a follow-up project (InduCat), which will make this technology ready for the market. Ten patent applications has been filled with basis on the results of the finished project.

Based on a literature survey, Co, Ni, and their alloys were identified as the possible candidates for being catalytically active and magnetic under reaction conditions. Thus, these materials were thoroughly characterized. The results suggested that both high cobalt and nickel content was ideal, so such materials were synthesized. These alloys were tested in a custom-built reactor setup, and showed on their own energy efficiencies of up to 8%. If a larger cobalt rod was added into the reactor, the efficiency increased to 60% because of the addition of the eddy currents to the energy transfer. This combined system can compete with electrolysis.

To achieve even higher performance, a better understanding of magnetic nanoparticles and industrial metalwork was required. Hence, a follow-up project was proposed and applied for. This project is defined together with DTU and Sintex that bring in additional required knowledge. The outcome of said follow-up project is to have the specifications for a prototype defined. Several patents were filled on the basis of the knowledge generated in the project, three patents were directly related to small-scale hydrogen production, and seven other were related to other processes where similar concepts and know-how could be applied.

1.4 Project objectives

The project started in February 2014 with an overall goal of evaluating the commercial potential of induction heating for hydrogen production by steam reforming application. The original Gantt diagram as presented in the original application for the project is presented in Figure 1.

Figure 1. Original Gantt diagram for the project as presented in the original application.

Unfortunately, the project was initially delayed due to negotiations over the collaboration agreement, which meant that the actual work on the project did not start before the summer of 2014. Despite this initial delay, the project quickly caught up, and before the end of 2014, suitable candidates for magnetic susceptible catalysts beds had already been identified and synthesized, and WP1 was well on track. This enabled that scaling of the test rig was done on time to meet M0 according to the plan.

WP2 had similarly caught up before the end of 2014, and a test setup was established for actual steam reforming tests at DTI prior to the summer of 2015. This setup fulfilled both M1 and M2.

The new setup enabled testing of different configurations of catalysts susceptors and from this point enabled progress in WP1, WP2, and WP3 in due time. The work performed on the setup had produced results of a sufficient quality to support considerations of efficiency and scale-up, which made progression on building a larger demonstration unit redundant (WP3). This work was stalled, and instead work was focused on developing an initial process configuration. This showed that the technology could fit into the known technology from classical steam reforming and it was at the given time concluded that experimental work on testing required gas clean-up etc. would not be needed, but simply utilization of Haldor Topsoe's already existing portfolio of gas cleaning unit operations would be sufficient. Practically, WP4 and WP5 had merged into a combined work effort on scale-up consideration from a pure engineering perspective.

The continued work on WP1, WP2, and WP3 during 2016 gave positive results on energy efficiency, stability of the catalytic system, and start-up times. On the basis of the progress in this period, it was agreed with EUDP to extent the project to the end of 2016 instead of August. Throughout 2016, M3 and M4 were therefore both met on time. By the end of 2016, results had been produced of a sufficient quality to show that the energy efficiency of the technology made the process competitive with electrolysis (considered as the direct benchmark) for small-scale hydrogen production to fulfill CM2.

The large prospect of the technology realized in the second period of the project gave interest for further work in the area and it was decided to open up the project and include more expertise to better the many technical aspects of the project. Instead of going directly for demonstration of the technology on a larger scale, it was therefore pursued to extend the research project for an additional period, but assisted by expertise from DTU on magnetism and surface catalysis, and Sintex A/S on magnetic materials and processing of these. This project was granted by Innovationsfonden and started in the closing stage of the current project. In the

beginning of 2017, the project on developing induction-heated steam reforming stands stronger than ever and appears as a prospective route for small-scale hydrogen plants. This choice means that the process is not ready for commercialization yet and contacting potential end users are therefore postponed (CM1) until a more final configuration has been decided upon. Insight into the needs of one hydrogen-consuming industry have been gained as Sintex A/S consume hydrogen in the production of sintered metal parts.

1.5 Project results and dissemination of results

1.5.1 Background

Induction heating is interesting in connection with reforming as heat transfer often will be the limiting factor in a traditional tubular reformer [1]. With induction, it could be possible to deliver heat directly to the catalyst. Additionally, induction heating offers a fast heating mechanism, which potentially could make start-up of a reforming plant relatively fast. The conceptual prospect is illustrated in Figure 2.
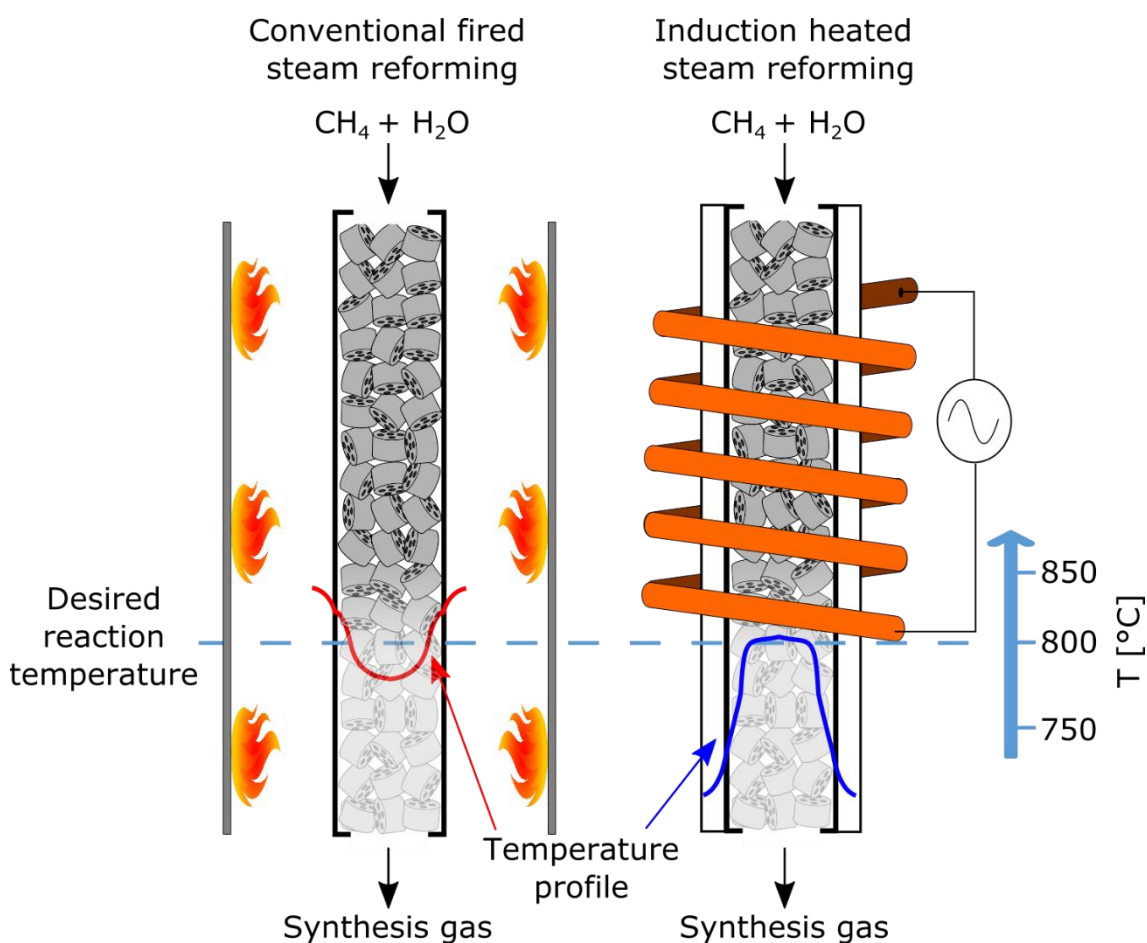
Figure 2. Conceptual idea of performing induction-heated steam reforming over conventional side-fired reforming.

Today, the decentralized market for hydrogen is often dependent on expensive distribution and storage of hydrogen [2]. As an alternative to this, induction-heated reforming could be envisioned as a small-scale hydrogen production technology, potentially with fast start-up for ad hoc hydrogen production and a heating system based on electricity and not a fired hot box. Today, hydrogen is most efficiently produced in large chemical plants from fossil fuels by the steam reforming reaction, where natural gas (methane) and steam are converted to hydrogen and carbon monoxide according to the following reaction scheme: $CH_4 + H_2O \rightleftharpoons 3H_2 + CO$ (reaction enthalpy $\Delta H° = 206.15$ kJ/mol) accompanied by the water gas shift reaction: $CO + H_2O \rightleftharpoons H_2 + CO_2$ ($\Delta H° = -41.16$ kJ/mol). As the reforming reaction is endothermic, heat is required for the reaction to proceed; the reaction energy is stored chemically in the produced gas. In order to achieve sufficiently high conversion of methane to hydrogen, the reactor is excessively heated to >850°C, typically by burning natural gas [1]. The timescale for turning on such

plants is in the order of several hours to days, due, especially, to the high temperature of the reactor. When at steady state, the plant typically operates at a continuous energy consumption rate for several months, and sometimes years.

As an alternative, facilitating steam reforming with induction heating of the catalyst would require that the catalyst is sufficiently active for the reforming reaction and at the same time susceptible for induction heating.

Two types of susceptor configurations were tested in this project. A catalytic susceptor configuration in which the catalytic nanoparticles are heated by induction; and a metal susceptor embedded in the catalyst. These configurations are shown in Figure 3.
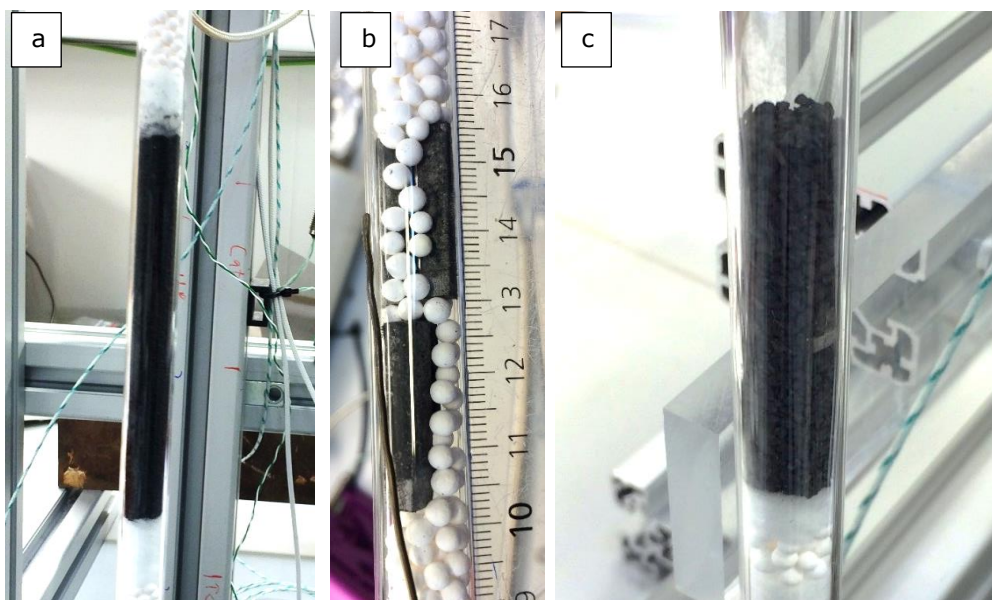
Figure 3. a) catalytic susceptor configuration where the nanoparticles in the catalyst is the susceptor; b) cobalt rods alone with inert particles; and c) metal susceptor embedded in the catalyst, i.e., cobalt rods embedded in the catalytic material.

1.5.2 Catalytic susceptor configuration

Finding active materials for steam reforming is already extensively investigated in the literature and can briefly be summarized by the density functional theory (DFT) work done by Jones et al. [3]. This is illustrated by the two-dimensional volcano plot shown in Figure 4, with the most active candidates being Ru, Rh, Ni, and Ir, decreasing in activity in that order.
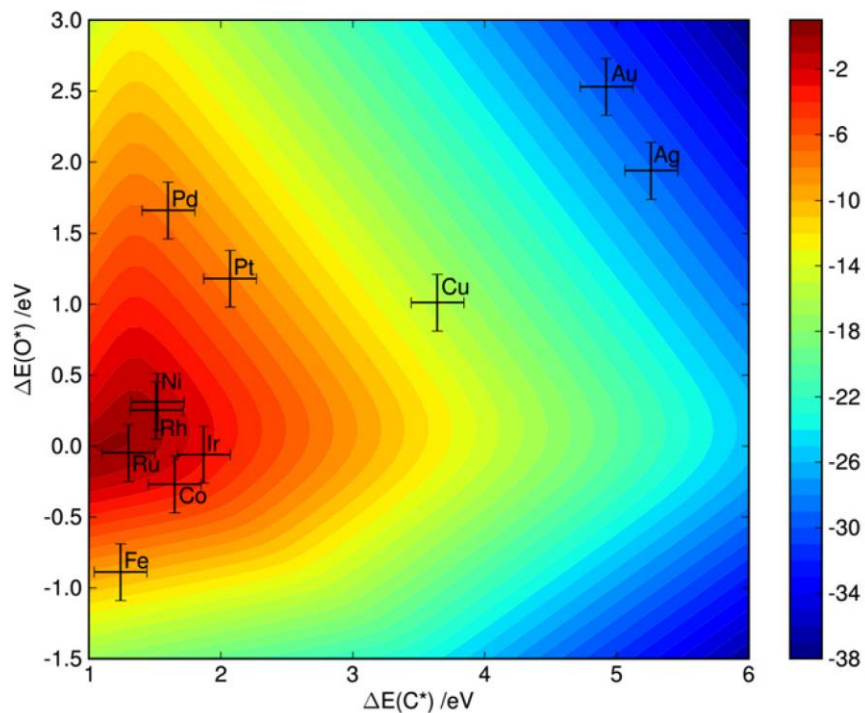
Figure 4. Two-dimensional volcano-curve of the TOF for SMR as a function of the oxygen and carbon adsorption energies. Relationship has been derived from DFT calculations. T = 500°C, p = 1 bar. Figure from Jones et al. [3].

Additionally, to make the catalyst susceptible to induction heating, it is favorable if the material is ferromagnetic (or ferrimagnetic/antiferromagnetic). The magnetic properties are very dependent on temperature because the thermal vibration of atoms increases with temperature. Over a given temperature, the thermal energy will be sufficiently large to overcome the cooperative ordering of the magnetic moments, which means that a ferromagnetic material will become paramagnetic. The temperature of this transition is material dependent and is known as the Curie temperature [4]. In practice, this is seen as a sudden drop in the saturation magnetization of a material as a function of temperature. Similar to the Curie temperature, also antiferromagnetic materials will become paramagnetic at elevated temperatures. This temperature is defined as the Néel temperature [4].

To have good induction heating under reforming conditions, material selection will be limited to materials with Curie/Néel temperatures higher than the operating conditions in the order of 900°C. Figure 5 compares the Curie temperature with the Néel temperature of pure elements that are either ferromagnetic or antiferromagnetic. Most elements cannot maintain a magnetic moment on their own at temperatures above 100°C. Only Ni, Fe, and Co can be used for higher temperature application, with Curie temperatures of 354°C, 770°C, and 1115°C, respectively.
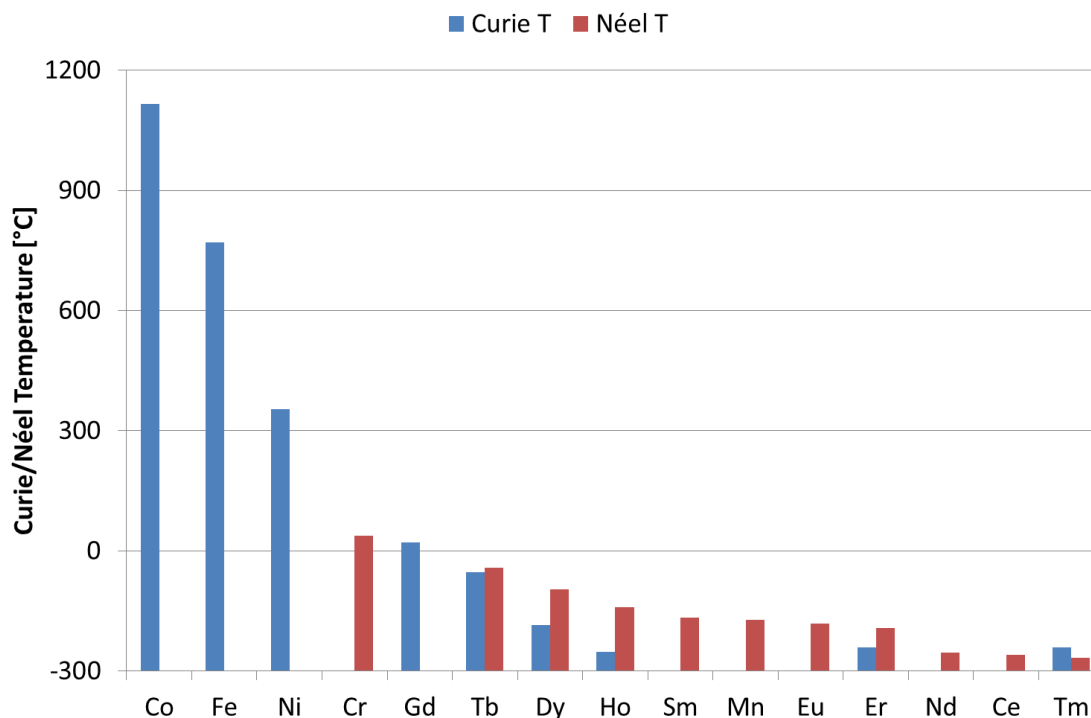
Figure 5. The Curie and Néel temperatures of elements having magnetic properties. Data from [5].

Compounds containing one or several of the different (anti)ferromagnetic elements will usually have a Curie temperature somewhere in between the Curie temperatures of the bulk compounds.

In summary, a catalyst for induction-heated reforming should ideally fulfill the following criteria:

- Sufficient catalytic activity for the reforming reaction.
  - Materials as Ru, Rh, Ni, and Ir are among the best to achieve high activity.
- A Curie temperature ideally above 900°C.
  - Only Co as a pure element can achieve this, but alloys with Co are also a possibility.
- A high hysteresis heating.

It seems evident that a catalyst for induction-heated reforming should at least contain some cobalt to enable inductive heating at high temperatures. However, the steam reforming activity of cobalt has previously been shown to be low [6]. A candidate for induction-heated reforming could therefore be a system based on both Co and Ni. Alloys of Co and Ni have previously shown decent activity for reforming [6].

Overall, a catalytic system of Ni and Co was identified as a prospective system for facilitating induction-heated catalytic steam reforming and chosen as starting point in the development work. The NiCo catalyst was synthesized in a variety of Ni and Co loadings on a commercial support material made of $MgAl_2O_4$ supplied by Haldor Topsoe A/S.

Initially, an activity analysis was made on the $NiCo/MgAl_2O_4$ catalyst, analyzing the impact on the Ni and Co content on the catalyst. This is summarized in Figure 6 on the basis of turnover frequencies (TOF) as a function of the Ni loading in the catalyst samples. The TOF was evaluated as the reaction rate relative to the total amount of metal surface sites. Increasing the Ni loading had a positive effect on the TOF as the series with roughly constant combined load of Ni and Co had a very apparent increasing pattern as a function of nickel content. In this evaluation, a sample with only cobalt displayed very limited activity.
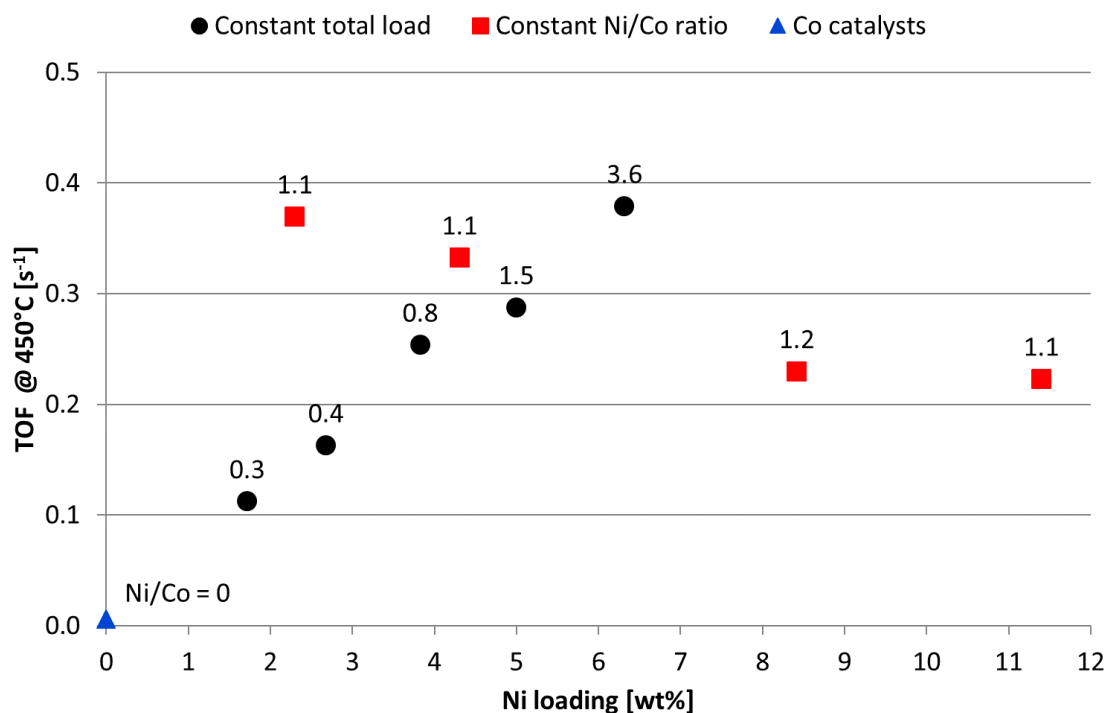
Figure 6. Activity of fresh NiCo/MgAl$_2$O$_4$ catalysts normalized to TOF as a function of Ni loading. Series of constant combined total load of Ni and Co of ca. 10 wt % is shown together with a series of roughly constant Ni/Co ratio but at increasing total load (ca. 5–25 wt %). Measurements was made using S/C=4.1, H$_2$O/H$_2$=10, T=450°C, P=1.2 bar.

Increasing the total loading (Constant Ni/Co ratio) gave a lower TOF. This is because the low loading resulted in better dispersion of the active metals and therefore a lower particle size. As the reforming reaction is structure sensitive, a lower particle size will result in a larger fraction of exposed low coordinated sites [1].

Overall, the activity analysis showed that nickel was essential for the catalytic activity, where cobalt appeared to, at most, play a minor role.

To investigate the magnetic properties of the NiCo/MgAl$_2$O$_4$ catalyst, a series of in situ magnetometer measurements was made by Michael Claeys at University of Cape Town on their custom-built magnetometer [7, 8]. In the measurements, the saturation magnetization was followed as a function of temperature, the hysteresis loss curve was measured prior to and after the temperature profile, and the hysteresis loss and coercive force were quantified from the hysteresis curve. Also, pure MgAl$_2$O$_4$ was investigated, verifying that the support did not have any ferromagnetic characteristics and did not interfere in the measurements.

The saturation magnetization of a NiCo/MgAl$_2$O$_4$ catalyst with 4.0 wt % Co and 4.5 wt % Ni is shown in Figure 7 as a function of temperature. The saturation magnetization decreased slowly as a function of temperature by ca. 35% from 50°C to 700°C. The residual saturation magnetization even at 700°C shows that the final Curie temperature of the material is (somewhat) higher than the magnetometer temperature limit of 700°C.
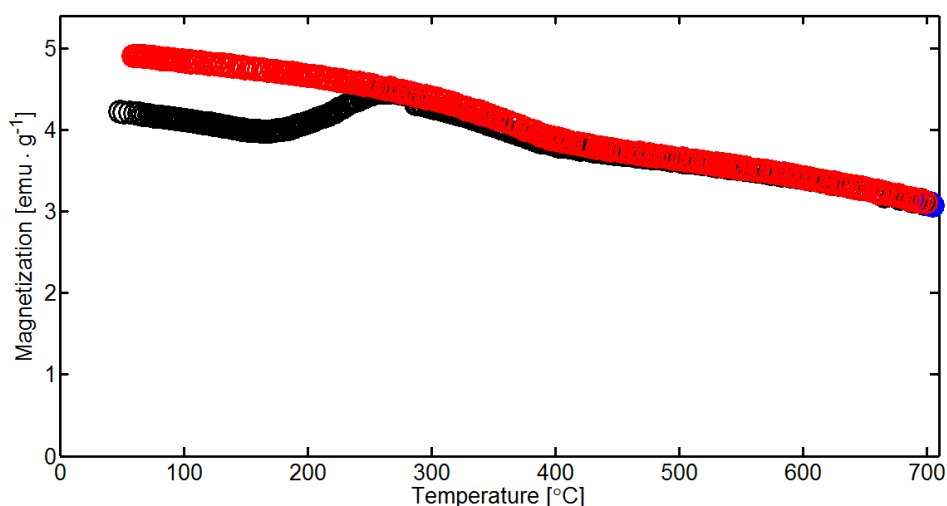
Figure 7. Saturation magnetization of NiCo/MgAl$_2$O$_4$ catalyst with 4.0 wt % Co and 4.5 wt % Ni at an external field strength of 2 T as a function of temperature during ramp up (**o**), holding (**o**), and cool down (**o**). Heating rate: 2°C/min, feed gas: 100 Nml/min H$_2$ and 100 Nml/min Ar.

During heating, an increase in the saturation magnetization was observed just above 200°C, which correlates with re-reduction of the passivated catalyst sample. Especially transformation of cobalt oxide species to metallic cobalt will have a pronounced influence on the saturation magnetization, as this means transformation from antiferromagnetic CoO/Co$_3$O$_4$ to ferromagnetic Co. During cool down, the same bend was not seen, which strengthens the argument of the behavior due to reduction.

Due to the re-reduction of the sample during the measurement, the size of the hysteresis loop measured after cooling was also larger than that measured before ramping, as shown in Figure 8.
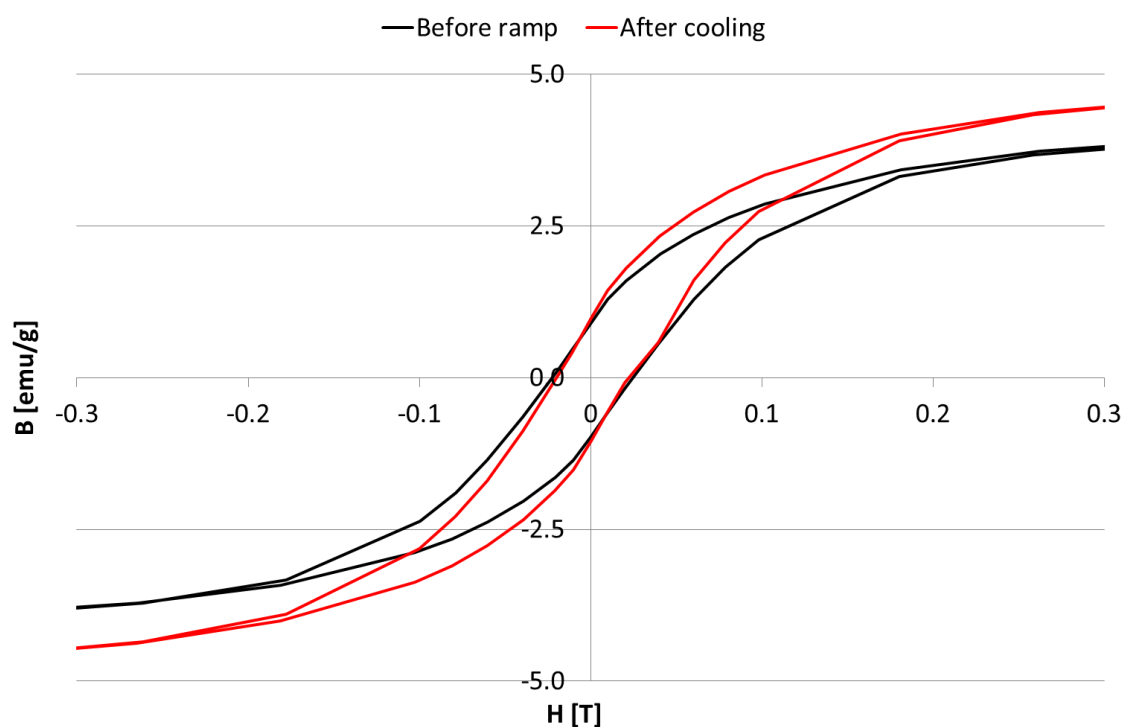
Figure 8. Hysteresis loop of a NiCo/MgAl$_2$O$_4$ catalyst at 50°C before and after the ramp experiment shown in Figure 7. Magnetic field: -2 to 2 T, temperature: 50°C, feed gas: 100 Nml/min H$_2$ and 100 Nml/min Ar.

The hysteresis curve was measured on a series of catalysts with different Ni and Co loading, which showed that the hysteresis loss increases with increasing cobalt content, as illustrated in Figure 9. Strikingly, W_h scaled practically linear as a function of the cobalt loading. Cobalt therefore appears to be the major contributor to the hysteresis loss, even at 50°C where the analysis was done, and nickel still is ferromagnetic.
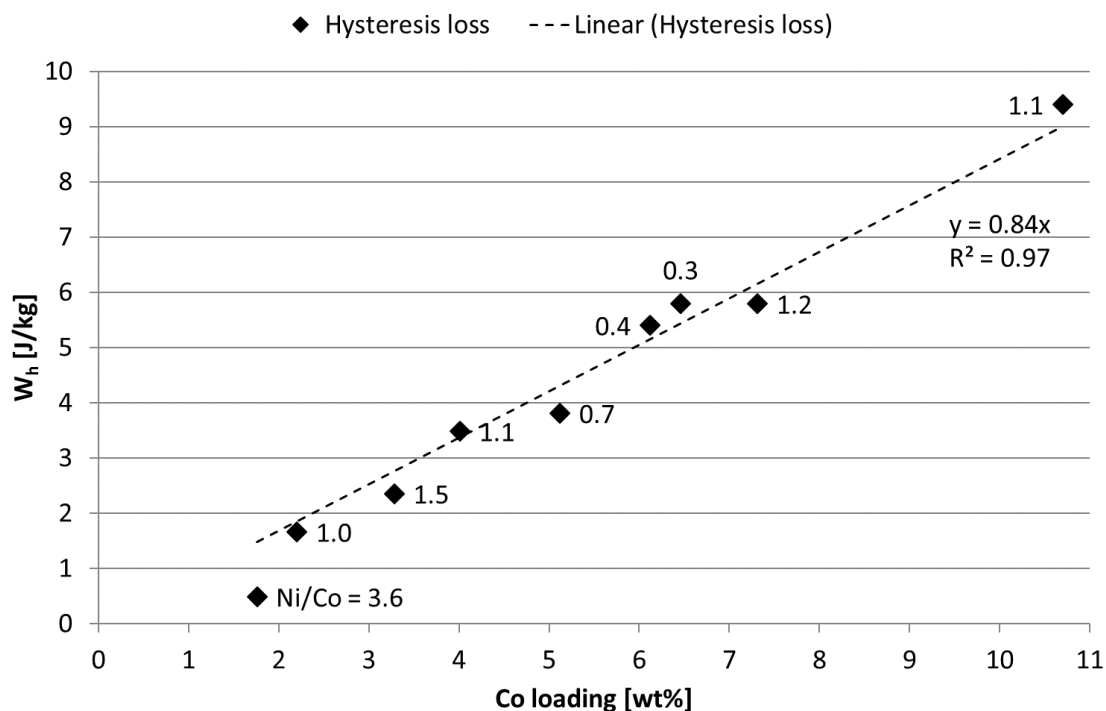

Figure 9. Hysteresis loss of NiCo/MgAl₂O₄ catalysts as a function of Co loading. Magnetic field cycled from -2 T to 2 T, temperature: 50°C, feed gas: 100 Nml/min H₂ and 100 Nml/min Ar.

To actually test the concept, an induction-heated bench-scale setup was established at DTI. The setup is illustrated in Figure 10. The setup is equipped with feed supplies for methane, hydrogen, and water. The water is evaporated prior to mixing with the methane and hydrogen feeds. At the frontend of the setup (until the reactor), the pipes are traced to keep a gas phase temperature of ca. 200°C to maintain the water in the gas phase.
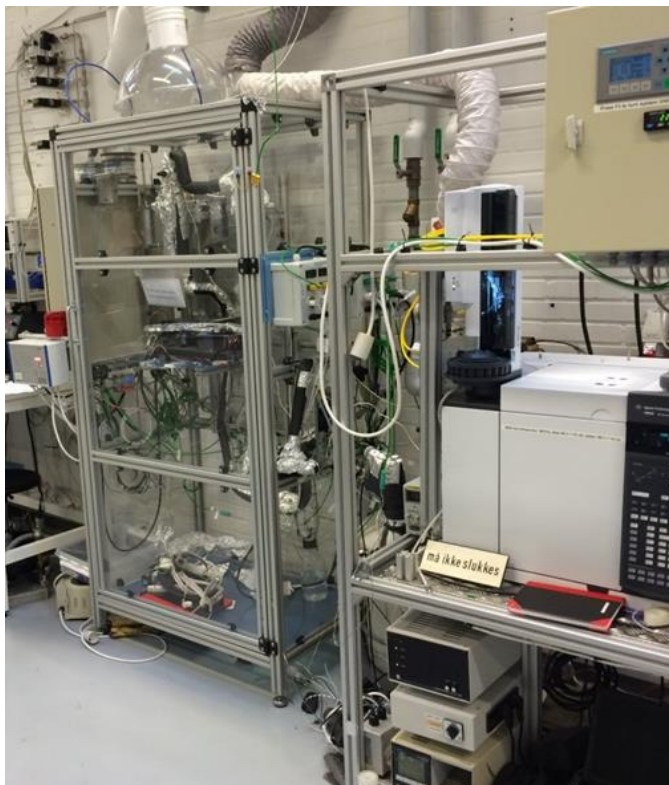
(a) Induction-heated reforming bench-scale setup
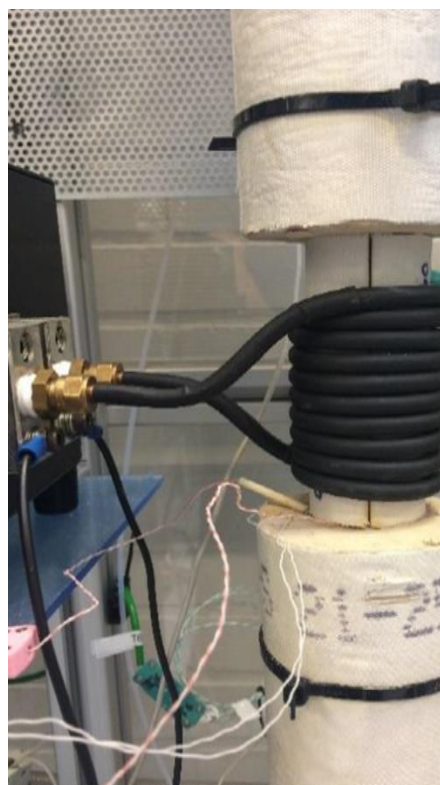
(b) Close-up of induction coil
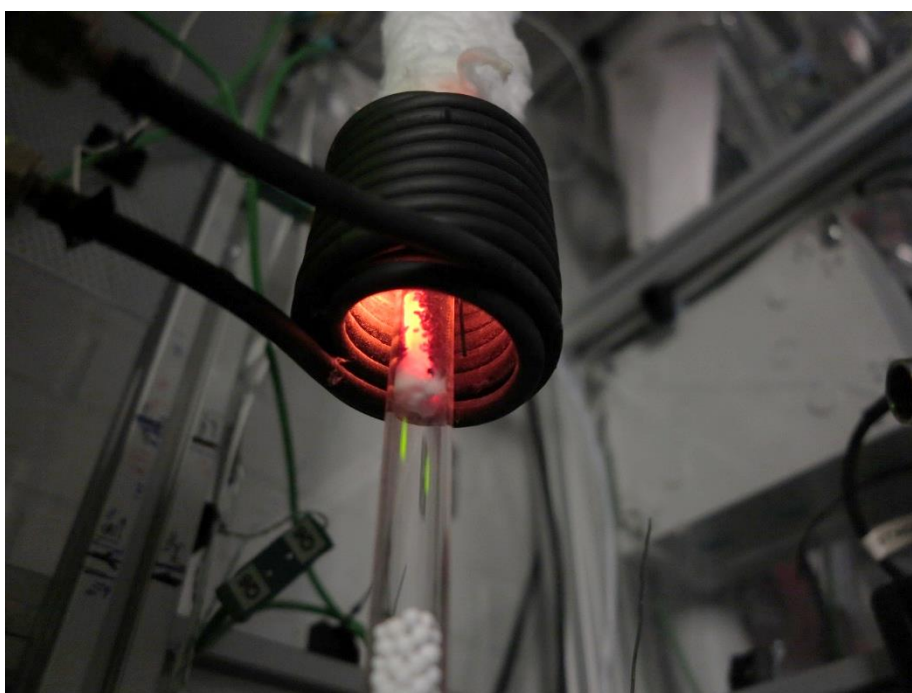
(c) Induction heating in operation

Figure 10. Induction-heated bench-scale setup. (a) is the full view of the setup with the setup in the left cabinet and the attached GC on the left, and (b) is a close up of the induction coil surrounding the reactor. (c) shows the induction-heated catalyst bed during operation without the insulation layer fitted.

The reactor is a glass reactor with an internal diameter of 13 mm. It is placed vertically and wrapped in insulation as illustrated in Figure 10(b). The induction coil is placed around the center of the reactor. This coil has a constant internal flow of cooling water to maintain its temperature close to room temperature.

The temperature of the reactor is measured before and after the coil, both on the inside and the outside of the reactor (roughly indicated in Figure 10(b)), but due to the interference of

the magnetic field, an actual temperature measurement of the catalyst bed was not possible to obtain in the experiments.

The induction heater supplying the alternating magnetic field for the induction coil is an Ultra-flex unit delivering an alternating current at 55.7 kHz at a magnetic field in the order of 0.01–0.1 T, depending on the power output.

After the reactor, the water is condensed and the dried gas is sent to analysis using a gas chromatograph. Gas-phase analysis is performed at ca. eight-minute intervals. Also, an online mass spectrometer was fitted for some of the experiments to achieve a higher time resolution. In a typical experiment, the catalyst was loaded in the middle of the reactor in the induction field. The catalyst was initially reduced in pure hydrogen at temperatures of ca. 400–500°C. After reduction, the activity of the catalyst was investigated using a typical gas mixture of 29.7% methane, 59.5% water, and 10.8% hydrogen, corresponding to a steam-to-carbon ratio (S/C) of 2. In all experiments, the pressure was 0–0.5 barg in the catalyst bed. During the experiment, both total flow and total power output of the induction heater were varied while following the impact of these parameters on the conversion of methane.

The performance of the $NiCo/MgAl_2O_4$ catalyst was evaluated in an experiment where it was loaded along the entire length of the coil. In this configuration, a series of power and total flow variations were performed. Figure 11 shows the conversion of methane and the equilibrium temperature for the steam reforming reaction as a function of power for series with different total flows. These results verify the concept of performing steam reforming with induction as the only heat source, as high conversions of methane and heating to above 800°C was achieved in the catalyst. At the lowest flows (10 Nl/h, 20 Nl/h, and maybe also 30 Nl/h), the equilibrium temperature leveled out at high power output because almost complete conversion of methane was achieved.
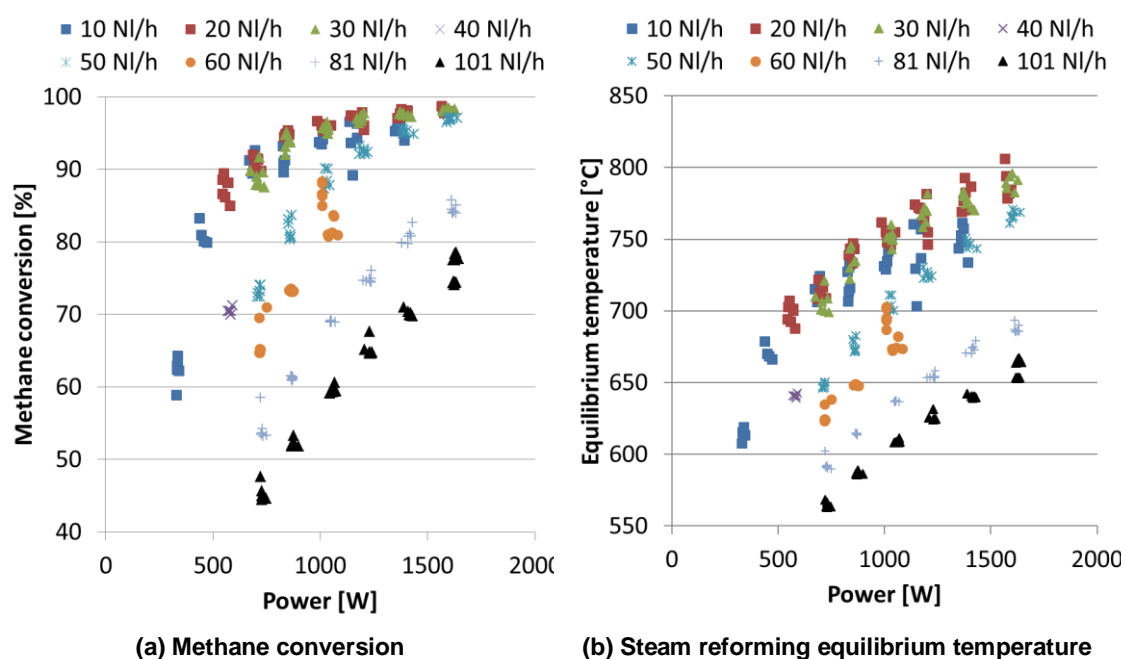

(a) Methane conversion   (b) Steam reforming equilibrium temperature

Figure 11. Conversion of methane (a) and equilibrium temperature of the steam reforming reaction (b) for a gas treated over a $NiCo/MgAl_2O_4$ catalyst as a function of power output of the induction heater and at different total flow rate series. Inlet temperature ≈ 200°C, S/C = 2, y_{H2} = 11%, P ≈ 0 barg.

Calculating the energy transfer efficiency of the system, a general low energy transfer to the catalyst bed was observed during the experiment as it was 8% in the best-case scenario, as shown in Figure 12. The best efficiency was obtained in a case with a relatively low conversion of methane of 45% at the highest flow rate (101 Nl/h). Increasing the power, and thereby the conversion, or lowering the flow in both cases resulted in a lower efficiency. The efficiency dropped when the reaction approached complete conversion where a sudden drop was observed above 90–95% conversion. At the high conversion, the magnetic field is inefficiently

utilized as energy no longer can be transferred to the chemical reaction but instead ends up heating the susceptor alone.
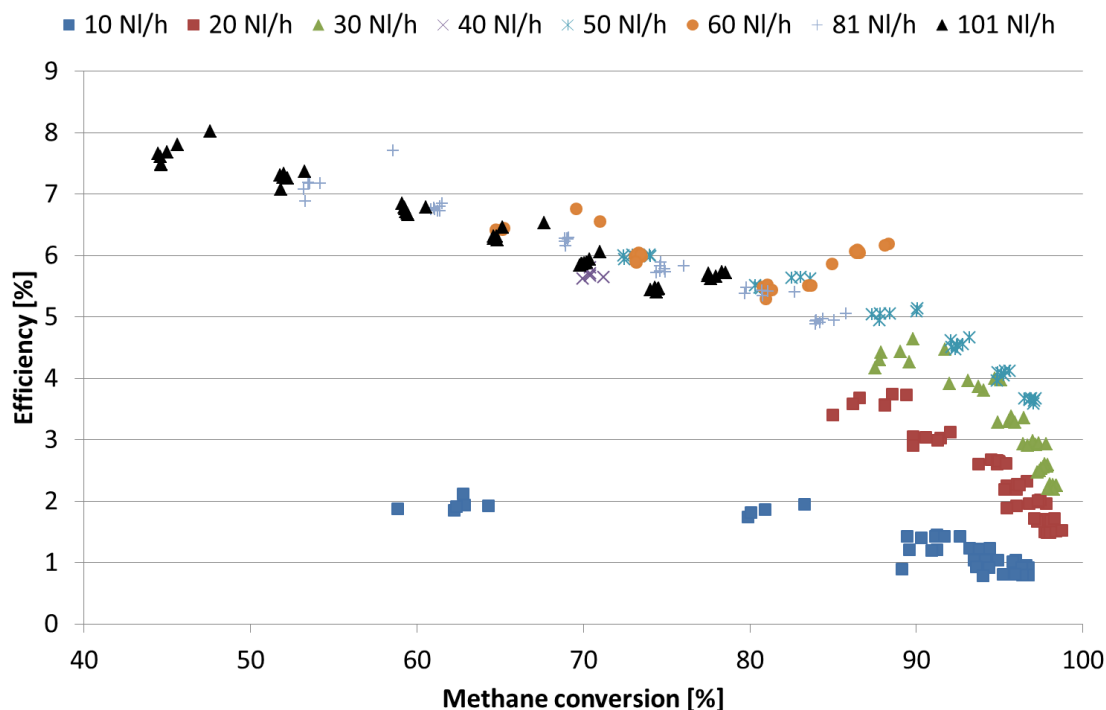

Figure 12. Energy transfer efficiency of the induction-heated process over a NiCo/MgAl$_2$O$_4$ catalyst as a function of methane conversion at different total flow rate series. Inlet temperature ≈ 200°C, S/C = 2, y_{H2} = 11%, P ≈ 0 barg.

Overall, high conversion of methane was enabled using the NiCo/ MgAl$_2$O$_4$ catalyst as susceptor alone, but at a very low efficiency. The receiving part of the NiCo/MgAl$_2$O$_4$ is limited to the Ni-Co nanoparticles alone, and these particles have a very small dimension. This practically precludes heating by eddy currents and thus only allows heating in the nanoparticles by hysteresis. Consequently, the low efficiency of the NiCo/MgAl$_2$O$_4$ catalysts is probably an effect of the high reliability of hysteresis heating where a strong magnetic field is required, which is produced from a high current in the electrical components. This results in a significant heat loss in the surrounding equipment.

Increasing the cobalt loading of the catalyst did indicate a slight improvement in the energy transfer efficiency, as illustrated by the best-case scenarios in Table 1. However, the absolute changes were small.

At the start of this project, few examples of induction-heated catalysis had been reported. Mentioning a few, induction-heated catalysis was used in conjunction with magnetic nanoparticles in the pioneering work done by Ceykan *et al.* [9] for the Suzuki–Miyaura and Heck coupling reactions in a liquid-phase organic synthesis flow reactor. Chatterjee *et al.* [10] showed how induction heating could be used for fast and isothermal heating of a microreactor system loaded with nickel ferrite microparticles in the 80–100°C temperature regime. Bordet *et al.* [11] used supported catalytic iron carbide nanoparticles to run the exothermic Sabatier reaction, converting carbon dioxide and hydrogen into methane and water. However, no example of high-temperature endothermic induction-heated catalysis had been reported, as in the present case, and achieving operating temperatures of 800°C directly in the catalytic system is a breakthrough. These novel results have been summarized in an article that is currently being processed for publication in a scientific journal.

1.5.3 Metal susceptor embedded in catalyst configuration

The experiments with the catalyst susceptor alone demonstrated that induction heating most efficiently is facilitated if both eddy currents and hysteresis heating is possible. Thus, moving away from the catalyst-only configurations, the overall best consumption figures were achieved by having a core of ferromagnetic material surrounded by catalyst (see Figure 3), as summarized by the experimental data in Figure 13 showing the energy transfer efficiency for

a system of NiCo/MgAl$_2$O$_4$ loaded around a core of cobalt rods. In this case, more than 50% energy transfer efficiency could be achieved at methane conversions above 90%. In this configuration, the loss was primarily found to relate to the laboratory equipment used, which is not designed for energy optimization.
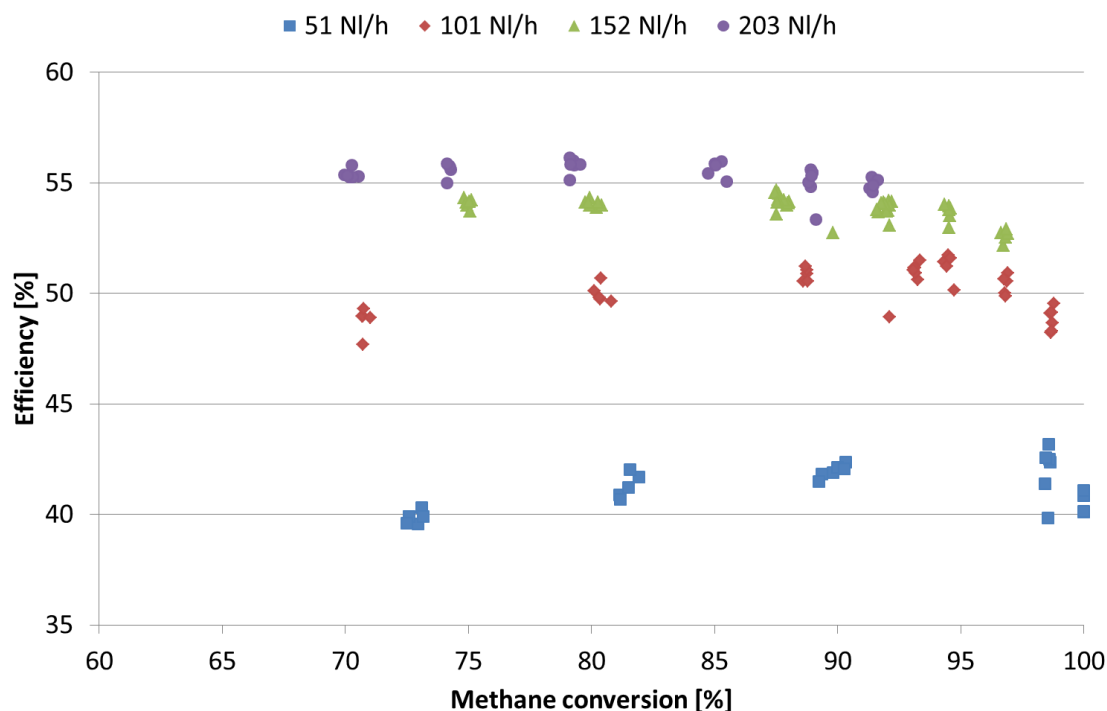

Figure 13. Energy transfer efficiency of the induction-heated process over a catalyst bed of NiCo/MgAl$_2$O$_4$ loaded around cobalt rods as a function of methane conversion at different total flow rate series. Inlet temperature ≈ 200°C, S/C = 2, y_{H2} = 11%, P ≈ 0 barg.

In this configuration, the choice of catalyst and susceptor can be chosen irrespectively of each other, opening up for the use of metallic cobalt as a core with its high Curie temperature. In total, three configurations, NiCo/MgAl$_2$O$_4$ + Alnico, NiCo/MgAl$_2$O$_4$ + cobalt, and a Haldor Topsoe A/S commercial reforming catalyst + cobalt, were tested. Table 1 summarizes performance data for the different configurations. This showed a clear benefit of using a cobalt core rather than an Alnico core due to the higher Curie temperature of cobalt, 1115°C relative to 850°C, respectively. Additionally, a small synergy effect could be achieved by using a ferromagnetic catalyst around the metal core, as slightly better performance data were obtained when using NiCo/MgAl$_2$O$_4$ + cobalt relative to the commercial catalyst + cobalt (cf. Table 1). Harvesting the full potential of this synergy would require further optimization. To evaluate stability, the NiCo/MgAl$_2$O$_4$ + cobalt system was run for 504 hours at constant input parameters with 92% methane conversion without observing any change in conversion or temperatures.

Table 1. Comparison between the investigated configurations showing maximum obtained methane conversion, equilibrium temperature, and electrical efficiency chosen across all data for the configuration and a best-case dataset (best production figures at close to 95% conversion).

Configuration	Maximum			Best case		
	X [%]	Eq. T [°C]	η [%]	X [%]	Eq. T [°C]	η [%]
Ni(13)Co(9)/MgAl$_2$O$_4$	98	806	8.0	95	747	3.9
Ni(9)Co(14)/MgAl$_2$O$_4$	99	806	6.0	95	743	4.8
Ni(9)Co(20)/MgAl$_2$O$_4$	99	807	5.8	95	743	5.1
NiCo/ MgAl$_2$O$_4$+Alnico	100	>810*	48	95	766	43
NiCo/ MgAl$_2$O$_4$+cobalt	100	>810*	56	95	736	54
Commercial catalyst+cobalt	100	>810*	54	96	741	52

* The high conversion of methane makes this uncertain.

To evaluate stability, the NiCo/MgAl$_2$O$_4$+cobalt system was run for 504 hours at constant input parameters with 92% methane conversion without observing any change in conversion or temperatures. As a first analysis, the system therefore appears stable during prolonged operation.

Start-up was additionally tested in the configuration with the NiCo/MgAl$_2$O$_4$ catalyst loaded around a Co core. In this test, the change in the gas composition was followed as a function of time on an online mass spectrometer and the results are shown in Figure 14. This analysis revealed that the given laboratory setup could be started from a dwelling stage at around 200°C to steady state at >90% conversion of methane in a time frame close to 3 min. This fast response opens for flexible use of the technology.
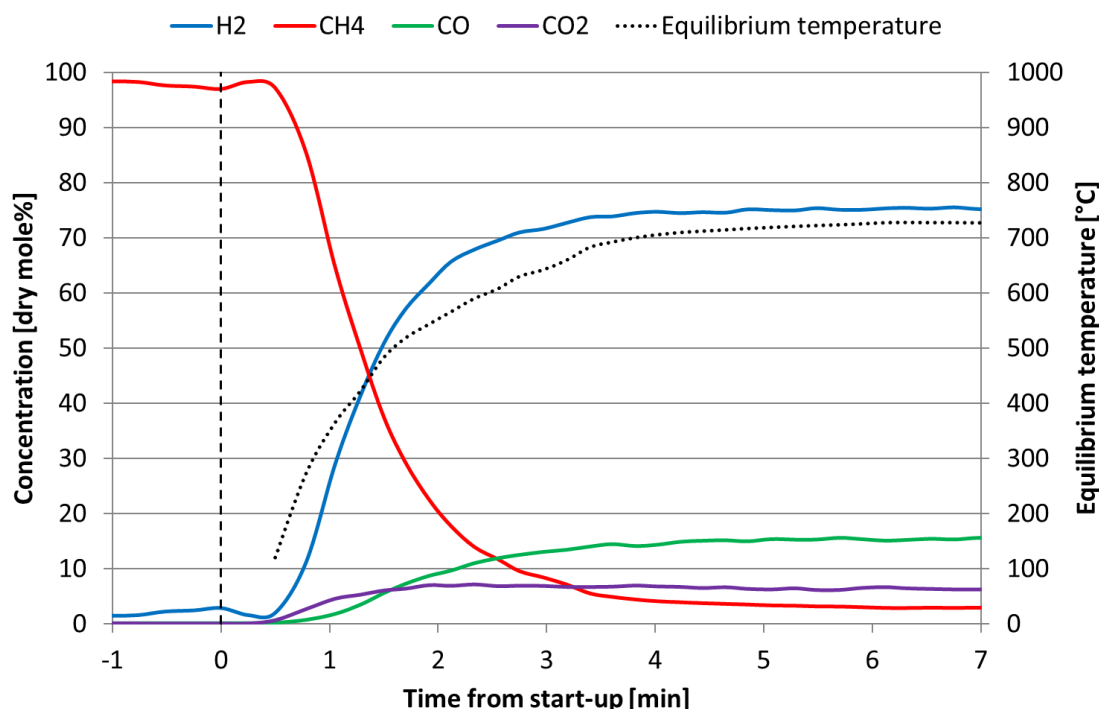

Figure 14. Changes in gas composition during start-up of laboratory setup of the induction-heated process over a catalyst bed of NiCo/MgAl$_2$O$_4$ loaded around cobalt rods. Inlet temperature ≈ 200°C, S/C = 2, y_{H2} = 11%, P ≈ 0 barg.

1.5.4   Consumption figures and benchmarking

The overall best consumption figures were achieved in the configuration of NiCo/MgAl$_2$O$_4$ loaded around cobalt with a methane conversion of 95% at an efficiency of 54%, which is very promising at the current stage, also considering the limitations of the setup. To normalize and

compare the consumption figures of the different configurations, a summary of the energy relative to hydrogen production and methane consumption is shown in Figure 15. In the best case, the test unit used 1.9 kWh per Nm³ of hydrogen produced while consuming 0.29 mole CH_4 per mole of H_2 produced. For comparison, an industrial-scale electrolysis unit uses 4.9 kWh per Nm³ of hydrogen [12], and this technology must be considered as a direct benchmark, as this is also an electrically driven hydrogen production technology.
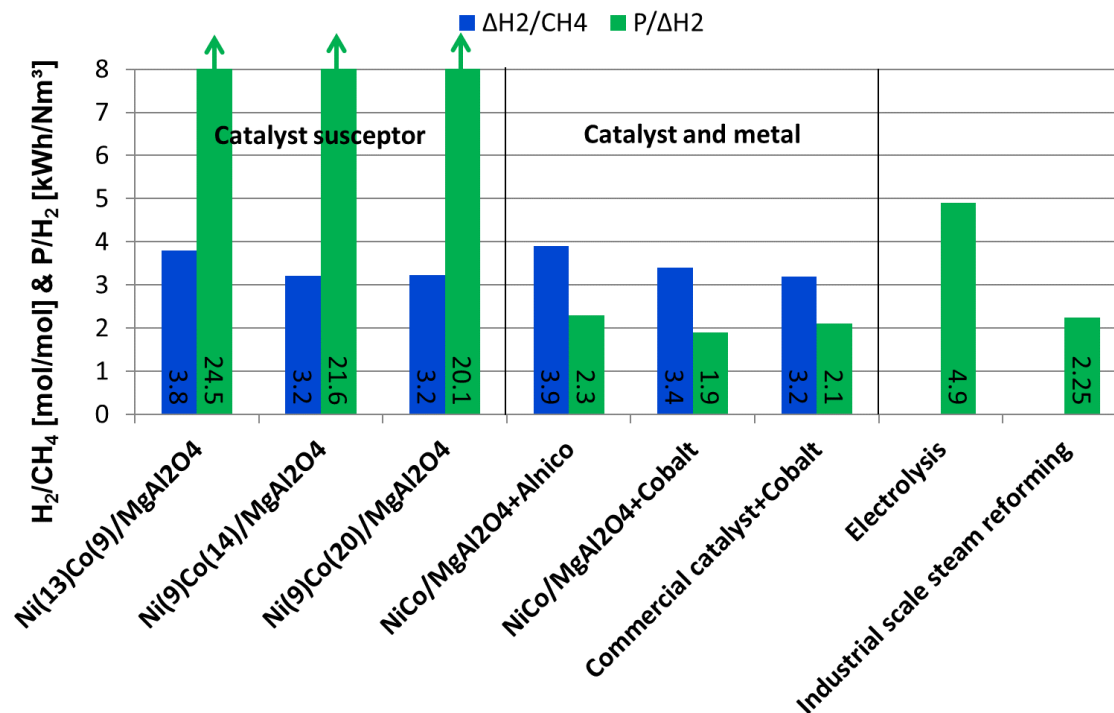
Figure 15. Consumption figures of different technologies at 95% methane conversion (if possible). $P/\Delta H_2$ is a measure of how much energy has been used by the induction oven to produce one Nm³ of hydrogen. Electrolysis is included as reference for electricity-based hydrogen production [12] and industrial scale steam reforming is included as reference of current state of the art [12].

Based on the consumption figures evaluated in the laboratory, the concept was transferred into a small-scale steam reforming unit design for better estimation of production costs. A general layout was analyzed that included a desulfurization section with an inlet temperature of 380°C and a prereforming section with an inlet temperature of 500°C. The actual reformer was an induction-heated unit with a given energy transfer efficiency (η). Downstream the reformer, a shift reactor was placed with an inlet temperature of 210°C, before water was separated in a flash separator at 35°C and hydrogen was refined in a PSA with an assumed separation ratio of 80%. The tail gas of the PSA was used for production of steam in a boiler. Heat exchangers were included between the different unit operations to make most use of waste heat from the reformer. A flowsheet of this process is given in Figure 16.
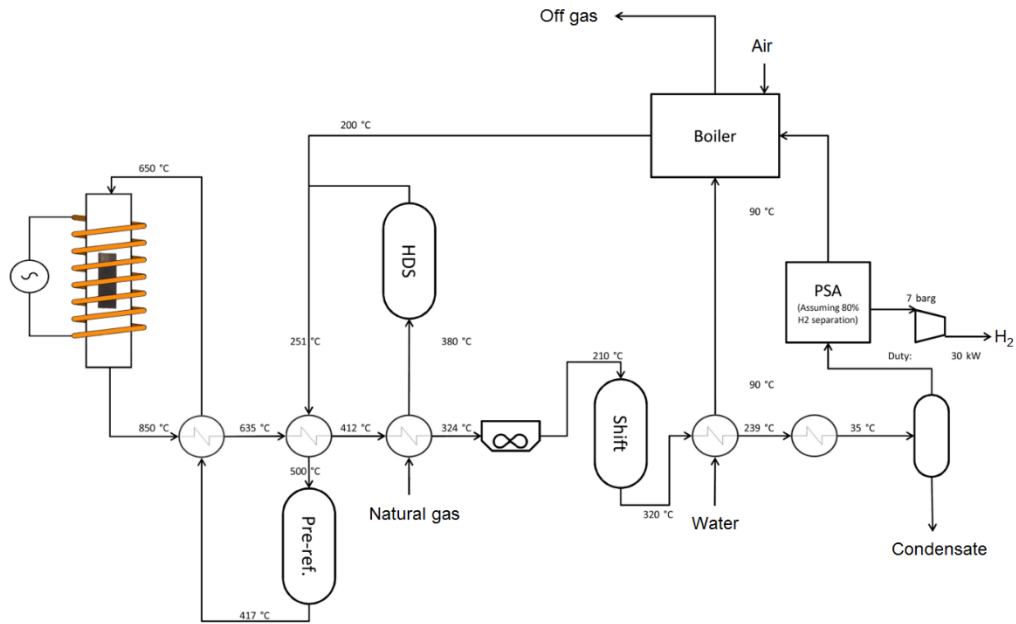
Figure 16. Example of flowsheet for induction-heated steam reforming.

The layout in Figure 16 was analyzed economically to make an assessment of the hydrogen price when including depreciation, operator costs, and other running costs. A plant of a capacity close to 700 Nm³/h hydrogen was simulated (see flowsheet in Figure 16), assuming a lifetime of 20 years for the plant, with 6000 h on stream per year (68% on-stream factor) and 1/3 of an operator maintaining the daily operation. Power consumption was calculated from consumption figures already calculated in the flowsheet and then adding 100 kW to cover other unspecified utilities. Obviously, the price of production of hydrogen by either induction-heated reforming or electrolysis will be significantly influenced by the price of electricity. In order to leave this as a more or less free variable, the production price was calculated as a function of electricity price for electrically heated reforming both in the induction-heated reforming case (with 60% energy transfer efficiency as obtained in the experiments, see Table 1) and compared with electrolysis, which is shown in Figure 17. For all three cases, upper and lower limits are shown. In the reforming cases, the lower limit corresponds to a low investment cost of USD 0.79 million and a low natural gas price of USD 0.359/Nm³, while the upper limit corresponds to a high investment cost of USD 2.26 million and a high natural gas price of USD 0.485/Nm³ (the natural gas price span was chosen on the basis of data from Eurostat [13]). These spans were chosen as at the given time it is uncertain what the actual production price for an induction-heated steam reforming unit would be. The upper and lower limits of the electrolysis price reflect the uncertainty span given in the report from the US Department of Energy where the end cost of hydrogen production was evaluated when evaluating the full lifetime of such plant [14].
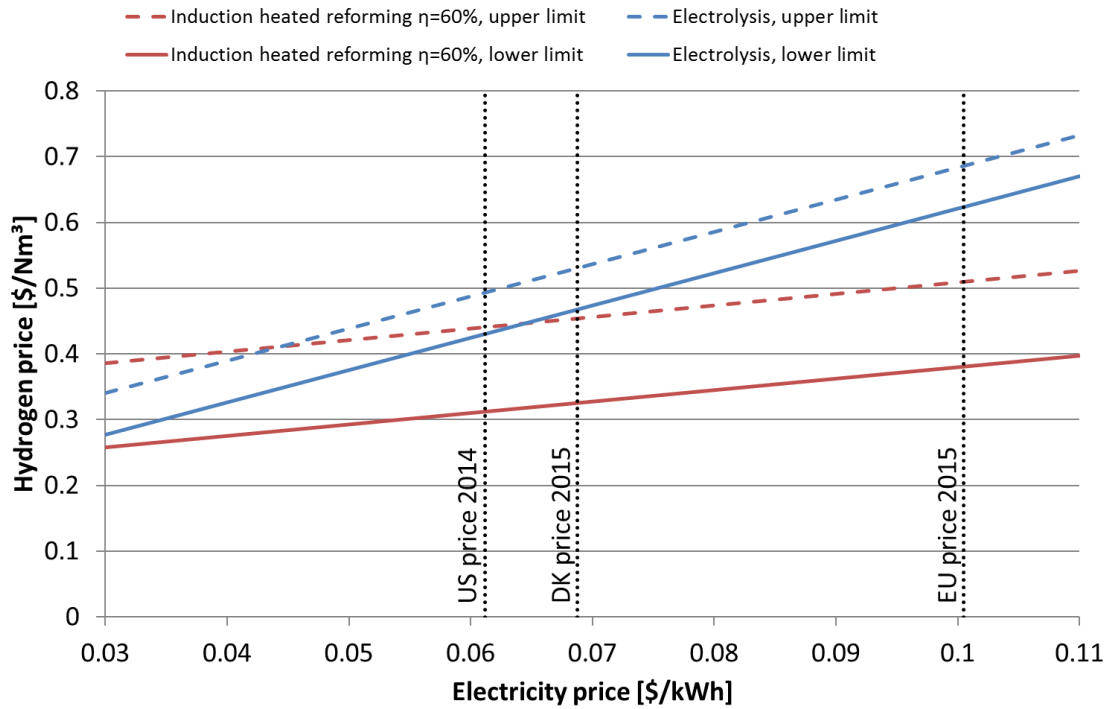
Figure 17. Price of hydrogen as a function of the electricity price.

The reforming case shows a wide span in the hydrogen price, which is due to the high uncertainty especially in the investment costs. Despite the span, induction-heated reforming shows lower hydrogen prices than electrolysis in a wide electricity price range, even at the upper limit. Looking at an average value, induction-heated reforming gives a lower hydrogen price than electrolysis, while the electricity price is above USD 0.034/kWh. For reference, the electricity price: in the US in 2014 (as used in the study of the US Department of Energy [14]) it was USD 0.061/kWh, in Denmark in 2015 it was USD 0.069/kWh [13], and in Europe on average in 2015 it was USD 0.101/kWh [13]. Thus, induction-heated reforming appears as the cheaper option for electricity-based hydrogen production in a current scenario.

Overall, the current evaluation of consumption figures shows that heating by induction appears as an attractive solution for electricity-based hydrogen production. However, despite these positive results, the concept is still not ready for commercialization. In the catalyst susceptor system, better efficiencies are required, as 5–6% is insufficient for any practical use. To overcome this, a catalytic system with a larger hysteresis curve needs to be developed, as the elongated nature of the $NiCo/MgAl_2O_4$ indicates a superparamagnetic like behavior (see Figure 8), which is not optimal for hysteresis heating. For the metal core embedded in catalyst system, a key concern observed during the test was a risk of metal dusting of the metal core (for information on metal dusting reference is made to [15, 16]), as a large temperature gradient properly exists between these. This issue will need to be addressed, as this would otherwise lead to erosion of the metal during prolonged operation.

Additionally, the current tests were all performed in a quartz reactor due to the shielding nature of most alloys, but this is not practically in a large-scale process. The shielding of an AC magnetic field inside a tube can be approximated by the following equation, if the wall thickness is much smaller than the diameter:

$$\frac{B_{out}}{B_{in}} = e^{-\sqrt{\pi \sigma \mu f} \, \Delta r}$$

B_{out} is the magnetic field outside the tube, and B_{in} is the magnetic field inside the tube. σ is the conductivity of the metal tube, μ is the magnetic permeability of the metal, f is the frequency of the magnetic field, and Δr is the wall thickness of the tube. Figure 18 shows attenuation of an AC magnetic field inside a metal tube. Theory and measurements are showing that a wall thickness of more than 1 mm is shielding a severe amount of magnetic field. How-

ever, to commercialize the system, it is desired to move the concept into pressurized equipment, which can be integrated into a larger process more easily. This requires a wall thickness of more than 1 mm, so a better reactor design will be made.
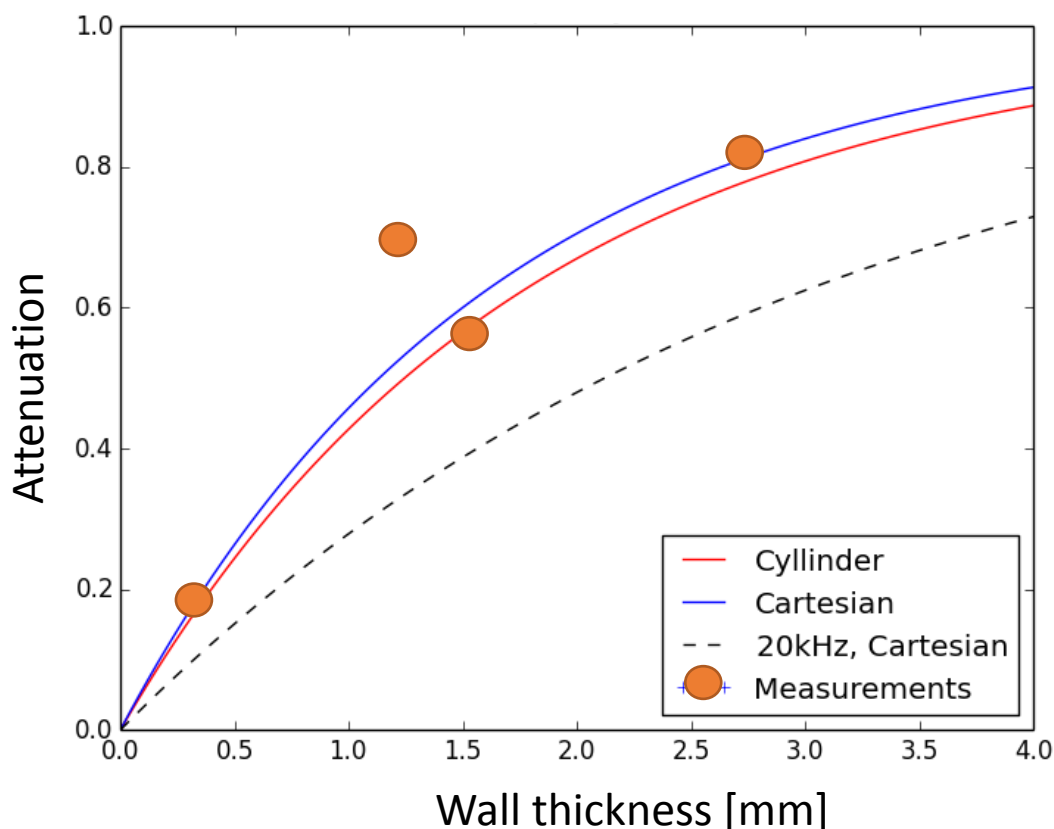

Figure 18. Study of the shielding effect as a function of wall thickness. Tube diameter is 20 mm, and σ is 0.76 μΩ m. The solid lines are at a frequency of 70 kHz, the dashed are at 20 kHz. The solution to the problem using cylindrical coordinates (red line) and assuming it is a plate (blue line) are similar at this ratio of thickness and tube diameter.

1.5.5 Dissemination of the project

At the end of the current project, despite the challenges, the project is at a positive standpoint and the concept looks promising for a future prospective solution for small-scale hydrogen production. The concept is not ready for commercialization yet, but instead, the project succeeded in continuing the work in a new research project where the participant group was increased to better tackle the diverse challenges faced, more on this in Section 1.6. The project expansion involves many additional people, including two new Ph.D. projects. In addition to the expanded project, a Ph.D. project was also established during the current project, where Morten Gotthold Vinum from Copenhagen University was hired into the project as a 1/3 Ph.D. student starting from March 2015; the other 2/3 were associated with other university activities. This Ph.D. project was funded by Haldor Topsoe A/S outside the present funding. The focus of this project was to build on the experience of the NiCo/MgAl$_2$O$_4$ catalyst system to synthesize an even better catalyst for induction-heated steam reforming.

The results, trends, and perspective of the project was presented by a poster November 10, 2016 on "Den Danske Brint- og Brændselscelledag" and in April 2017 on the meeting "Udvikling af fremtidige metoder til production af biobrændstoffer og dermed grønenergi" held by Ingeniørforeningen IDA. Additionally, an article is in process, which will be published in a scientific journal, and it describes the findings of the NiCo/MgAl$_2$O$_4$ catalyst.

1.6 Utilization of project results

The current project started from a conceptual idea, but made good progress on the technical development (as described in Section 1.6). The consumption figures achieved so far were very

promising (as summarized by Figure 17 and currently appears to be a prospective alternative to electrolysis-based hydrogen production). Given the large scale of the hydrogen market, the future prospect of the project remains large. However, as also evident from the description of the technical development work in Section 1.6, the concept still has room for improvement. Realizing this, it was decided in the closing stage of the project to widen the project and include additional participants to increase the expertise within the many areas the topic touches upon. Consequently, during 2016, a new project (InduCat) was established where the partners were expanded to also include DTU (for more fundamental research) and Sintex A/S (who brings key knowledge on metal processing) in addition to the original partner from DTI. This project is funded by Innovationsfonden with DKK 17.5 million and has a total budget of DKK 26.4 million. This project runs from May 2016 to 2020. The master plan of the project is to combine the expertise of Haldor Topsoe A/S on catalytic systems with that of Sintex A/S on shaped metallic structures, DTU on magnetic and catalytic nanoparticles, and DTI on induction systems, in order to realize a novel prototype of induction-heated catalytic system for hydrogen production as an end result. The key challenges that are addressed in the new project are:

1. Finding new and better catalytic systems with large hysteresis curve for direct induction-heated steam reforming. This task will primarily be done between DTU and Haldor Topsoe A/S.
2. Developing a reactor system to enable pressurized induction-heated catalysis. This task will primarily be lifted by DTI, but in collaboration with Haldor Topsoe A/S, DTU, and Sintex A/S.
3. Develop and design an induction coil that can supply a magnetic field for a prospective elongated catalytic bed. This will be done by DTI.
4. Understanding the temperature gradients in the induction-heated system, especially with bulk metallic structures inside the catalyst bed. This task will be led by computational fluid dynamic simulations at DTU, but assisted by DTI and Haldor Topsoe A/S.
5. Developing new and preferably hard magnetic materials. This will be done by Sintex A/S.

If the challenges listed above can be solved to a sufficient degree, it is believed that induction-heated steam reforming is a prospective solution in the future hydrogen market. By utilizing induction, we can transfer energy directly to the catalyst for steam reforming (as illustrated by Figure 2) and overcome the problems associated with transferring heat from a fired furnace through reactor walls to the catalyst, as seen in traditional steam reforming. This offers a route for a more compact reformer design, as the large furnace and accompanied waste heat management section are avoided, making it ideal for decentralized hydrogen production. By using induction heating, it is also possible to start and stop the reaction quickly (as illustrated by the results in Figure 14), hereby enabling production on demand or to follow availability of cheap excess energy from renewable sources.

The environmental benefits of hydrogen produced on the basis of induction-heated steam reforming include a smaller carbon footprint compared with standard steam reforming, as the heating can be facilitated by renewable energy sources, such as wind and solar power, versus the burning of fossil fuel. Furthermore, in the long run, induction-heated steam reforming can become independent of fossil fuels if the feedstock is methane from biogas. The proposed technology still produces CO_2 from the reaction, but the technology has the potential to integrate CO_2 capture, as one output product is a line of high-concentration CO_2.

The immediate market for this technology is decentralized hydrogen production. Steam reforming is cost-effective in large-scale plants, where hydrogen is produced on site for, e.g., ammonia/fertilizer production, methanol production, and oil refining. However, many industries do not have the required level of hydrogen consumption to make conventional steam reforming cost-effective and justify the large investment. These less intensive hydrogen-consuming industries range from glass and metal industries, performing heat treatments in reducing atmosphere, to the food industry, where vegetable oil is hydrogenated, to the semiconductor industry, where it is used as a carrier gas to remove residual oxygen. These industries must either invest in their own small and cost-inefficient hydrogen plant or buy hydrogen in pressurized bottles, which is impractical, as it requires extra energy, and results in safety concerns related to its transport.

Induction-heated steam reforming will have a competitive edge to existing technology in small-scale production of hydrogen as the consumption figures already at the current level seems

better than electrolysis (see Figure 17), which must be considered the current benchmark for small-scale hydrogen production.

As discussed in Section 1.5.2, no prior art exists within induction-heated catalysis above 300°C. Consequently, this has also opened for claiming novelty on the concepts investigated in the current project, and three patent applications were filed directly related to induction-heated steam reforming process. However, the development also laid the basis for filing seven additional patents on processes that could utilize the same concepts as learned during the project. This signifies that the work done in the current project not alone has given prospect on a concept for small-scale hydrogen production, but also has developed competencies for performing induction-heated endothermic chemistry on a more general level. If the development work in the new InduCat project succeeds, the results will to a large extent be readily usable for other processes and immediately give added value.

DTI has used the knowledge generated within this project to advice the Danish industry on efficiency of induction systems and related magnetic properties. DTI has developed the ability to measure constant and oscillating magnetic fields around a magnet or a coil, this is done by moving probes with a three-dimensional stage and measuring the field creating a three-dimensional model of the field. This is offered as a commercial service.

1.7 Project conclusion and perspective

We have shown that induction heating can be used to supply power to high-temperature catalytic reactions such as steam reforming and the energy transfer is so efficient that hydrogen can be produced at a price that can compete with electrolysis. Based on ongoing work in the InduCat project, further knowledge is gained, and 'soon after the project funded by Innovationsfonden, it is expected that an electrically heated hydrogen production unit can be built based on this EUDP project.

In the greater perspective, electrically driven chemical processes will become very relevant when we go toward a future on wind and solar power and biomass. The biomass available is limited and should not be wasted to supply process heat, when electric power from wind and solar power is available at a low price. By combining gas from biomass with extra hydrogen from electrolysis and induction-heated chemical reactors, we can produce bio-based fuels, chemicals, and polymers in an energy- and carbon-efficient way.

Annex
Relevant links

Annex

Manuscript: Peter Mølgaard Mortensen, Jakob Soland Engbæk, Søren Bastholm Vendelbo, Mikkel Fougt Hansen, and Martin Østberg, "Direct hysteresis heating of catalytic active Ni-Co nanoparticles as steam reforming catalyst", Submitted to Industrial & Engineering Chemistry Research, 2017.

References

[1] J.R. Rostrup-Nielsen, Steam Reforming, Handbook of heterogeneous catalysis, John Wiley & Sons, Inc., New York, 2008, pp. 2882-2905.

[2] C.W. Forsberg, Future hydrogen markets for large-scale hydrogen production systems, International Journal of Hydrogen Energy, 32 (2007) 431-439.

[3] G. Jones, J.G. Jakobsen, S.S. Shim, J. Kleis, M.P. Andersson, J. Rossmeisl, F. Abild-Pedersen, T. Bligaard, S. Helveg, B. Hinnemann, J.R. Rostrup-Nielsen, I. Chorkendorff, J. Sehested, J.K. Nørskov, First principles calculations and experimental insight into methane steam reforming over transition metal catalysts, J. Catal., 259 (2008) 147-160.

[4] W.D. Callister, D.G. Rethwisch, Magnetic Properties, Materials Science and Engineering: An Introduction, Wiley, Weinheim, 2013, pp. 803-837.

[5] H.P.R. Frederikse, Properties of magnetic materials, in: D.R. Lide (Ed.) CRC Handbook of Chemistry and Physics, CRC Press2009.

[6] J.R. Rostrup-Nielsen, Catalytic Steam Reforming, Springer1984.

[7] M. Claeys, E. van Steen, J.L. Visagie, J. van de Loosdrecht, A magnetometor, WO/2010/004419, 2009.

[8] N. Fischer, B. Clapham, T. Feltes, E. van Steen, M. Claeys, Size-Dependent Phase Transformation of Catalytically Active Nanoparticles Captured In Situ, Angew. Chem. Int. Ed. , 53 (2014) 1342-1345.

[9] S. Ceylan, C. Friese, C. Lammel, K. Mazac, A. Kirschning, Inductive Heating for Organic Synthesis by Using Functionalized Magnetic Nanoparticles Inside Microreactors, Angew. Chem. Int. Ed., 47 (2008) 8950-8953.

[10] S. Chatterjee, V. Degirmenci, F. Aiouache, E.V. Rebrov, Design of a radio frequency heated isothermal micro-trickle bed reactor, Chem. Eng. J., 243 (2014) 225-233.

[11] A. Bordet, L.-M. Lacroix, P.-F. Fazzini, J. Carrey, K. Soulantica, B. Chaudret, Magnetically Induced Continuous CO_2 Hydrogenation Using Composite Iron Carbide Nanoparticles of Exceptionally High Heating Power, Angew. Chem. Int. Ed., 55 (2016) 15894-15898.

[12] A. T-Raissi, D.L. Block, Hydrogen: Automotive fuel of the future, IEEE Power Energy M., 2 (2004) 40-45.

[13] Eurostat, Electricity prices by type of user, http://ec.europa.eu/eurostat/tgm/refreshTableAction.do?tab=table&plugin=1&pcode=ten00117&language=en.

[14] C. Ainscough, D. Peterson, E. Miller, Hydrogen Production Cost From PEM Electrolysis, Department of energy - United states of America, DOE Hydrogen and Fuel Cells Program Record, 2014.

[15] P.V.D.S. Gunawardana, T.T.M. Nguyen, J.C. Walmsley, H.J. Venvik, Initiation of Metal Dusting Corrosion in Conversion of Natural Gas to Syngas Studied under Industrially Relevant Conditions, Industrial & Engineering Chemistry Research, 53 (2014) 1794-1803.

[16] H.J. Grabke, Metal dusting, Materials and Corrosion, 54 (2003) 736-746.